Ann. Geophysicae 16, 1159–1168 (1998) © EGS – Springer-Verlag 1998

Annales Geophysicae

# Ion composition measurements and modelling at altitudes from 140 to 350 km using EISCAT measurements

**A. Litvine, W. Kofman, B. Cabrit**

Centre d'Etude des Phénomènes Aléatoires et Géophysiques, B.P. 46, F-38402 Saint Martin d'Hères, France
Fax: +33 04 76 82 63 84; e-mail: wlodek. kofman@lis.inpg.fr

Received: 6 November 1997 / Revised: 3 February 1998 / Accepted: 16 March 1998

**Abstract.** This work aims at processing the data of CP1 and CP2 programs of EISCAT ionospheric radar from 1987 to 1994 using the "full profile" method which allows to solve the "temperature-composition" ambiguity problem in the lower F region. The program of data analysis was developed in the CEPHAG in 1995–1996. To improve this program, we implemented another analytical function to model the ion composition profile. This new function better reflects the real profile of the composition. Secondly, we chose the best method to select the initial conditions for the "full profile" procedure. A statistical analysis of the results was made to obtain the averages of various parameters: electron concentration and temperature, ion temperature, composition and bulk velocity. The aim is to obtain models of the parameter behaviour defining the ion composition profiles : $z_{50}$ (transition altitude between atomic and molecular ions) and dz (width of the profile), for various seasons and for high and low solar activities. These models are then compared to other models. To explain the principal features of parameters $z_{50}$ and $dz$, we made an analysis of the processes leading to composition changes and related them to production and electron density profile. A new experimental model of ion composition is now available.

**Key words.** Auroral ionosphere · Ion chemistry and composition · Instruments and techniques · EISCAT

## 1 Introduction

The ion composition analysis in the F region is one of the most difficult problems in incoherent-scatter data analysis. In the F ionospheric region, between about 140 and 350 km, the transition between molecular and atomic ion composition occurs. This transition region varies depending on the geophysical conditions, and this is especially important for the auroral region, where the influence of energy inputs is large.

The incoherent-scatter spectrum depends on five parameters in this region:

$n_e$: electron density,
$T_e$ and $T_i$: electron and ion temperature,
$p$: ion composition,
$v_i$: ion velocity,

but the determination of five parameters simultaneously is very difficult, strongly depending on the signal-to-noise ratio and the method of measurements. For these reasons, one of the parameters, usually the ion composition, is fixed by the model. However, one can otherwise model the ion temperature by the Bates profile plus a correction term and model the ion composition (Oliver, 1979) and determine parameters. Different approaches were developed in order to derive the ion composition. This study was started at the beginning of incoherent-scatter work by Petit (1963) and Moorcroft (1964) and then improved by Lathuillère *et al.* (1983).

The analysis proposed by Lathuillère *et al.* (1983) consists in the determination of five parameters simultaneously. This is possible if the initial values chosen for the fit are not too far from the solution, and the data are integrated long enough. The method used to find the initial values consisted in making several fits on the measured ACF with a fixed composition ranging from only molecular ions to $O^+$ ions. The results of the fit for each assumed composition are the ionospheric parameters and the reduced chi-square parameter. The chi-square parameter is the reduced quadratic errors between the fit and the measured ACF and is usually used to check the quality of the fit. The parameters corresponding to the minimum value of chi-square are the closest ones to the solution and are chosen as initial values. Then a new fit was performed on all parameters including the composition. Each altitude is analysed independently.

*Correspondence to:* W. Kofman

There is an additional difficulty arising from the fact that there are often two minima in chi-square, very close to each other and occurring for composition values approximately symmetrical with respect to 0.5. So when minima were found, the two corresponding sets of initial values were used for the final fit and two possible values of composition were obtained for each ACF. The choice between these two sets of data was made afterwards, when all ACFs corresponding to all altitudes were reduced: one chooses the composition values when the profile fits the smoothest curve between 0 and 1 among all the possibilities. This processing strongly depends on the signal-to-noise ratio; the results are noisy and need averaging over a period of a few hours.

This method was applied on a few years of data (Lathuillère and Pibaret, 1992) and the authors determined a model of ion composition, especially for the altitude of the transition ($z_{50}$) between 50% of molecular and oxygen ions. In the last 5 years, several improvements in incoherent-scatter data analysis have occurred; see Holt *et al.* (1992), Lehtinen *et al.* (1996), Cabrit and Kofman (1996). All these works are based on the "full profile" approach which consists in fitting the whole set of scatter measurements at one time. This new analysis technique was proved to be the best possible way of reaching spatial resolution by directly fitting the set of lag profiles. It also has the advantage of leading to plasma parameters free from the gradient effects which usually corrupt standard analysis results (Holt *et al.* (1992).

In Cabrit and Kofman (1996) it was shown that the "full profile" technique can be efficiently used to extract independent information on the ion composition and on the ion temperature from incoherent-scatter data. The implementation was designed for EISCAT CP1 and CP2 data analysis. This means that fitted data are the gated lag profile cross-products, namely the plasma correlation functions. The first key point in Cabrit and Kofman's method is that one has to fit simultaneously high-resolution/low-signal (coded-pulse) and low-resolution/high-signal (long-pulse) data. The second key point is that one needs a suitable functional model of ion composition profile with a sufficient amount of flexibility to include all possible variations. The model used in the present study is different from the one presented in Cabrit and Kofman (1996). It will be described in the next chapter.

As we wanted to analyse the data measured by EISCAT over about 7 years, we had to automate the analysis in order to be able to do it relatively fast. As previous authors, we introduced two parameters significantly describing the composition profile; the $z_{50}$ parameters corresponding to the transition region between 50% of molecular and atomic ions and the width d$z$ of the transition defined in this paper as the altitude width between 10% and 90% of the composition. We studied the seasonal behaviour of the composition; the results of our analyses are shown and described precisely.

In the introduction, we want to emphasise the interesting behaviour, still needing a detailed explanation, of the $z_{50}$ and d$z$ parameters. $z_{50}$ and d$z$ show anticorrelation in summer and correlation in winter. This means that when $z_{50}$ decreases, d$z$ also decreases in winter and d$z$ has the opposite behaviour in summer. From our data, spring and autumn are transition periods between these two opposite behaviours.

The analysis of a large amount of data allows us to present two seasonal models for low and high solar activity for geophysical conditions without electric field in the field of view of the radar. The data analysis for perturbed geophysical conditions is much more difficult and still under study (Gaimard *et al.*, 1998). In fact, for high convection electric fields, the ion velocity distribution is no longer Maxwellian (Saint Maurice and Schunk, 1979; Hubert and Kinzelin, 1992) and this basic assumption in the data analysis is not valid. In addition, during high auroral activity, the fast time variability of the parameters prevents long integration time.

Our experimental model is important as an input to the polar ionospheric data bank, especially as this kind of data is very sparse. There are very few data concerning the ion composition because the satellite measurements in the F1 region of the ionosphere are difficult and rare.

## 2 Data analysis

### *2.1 Functional model of ionospheric parameters*

In our work we use the technique of "full profile" analysis which needs modelling, as a function of altitude, of the ionospheric parameters $n_e$, $T_e$, $T_i$, $p$ and $v_i$ by functions depending on a few parameters. The method used is fully described in Cabrit and Kofman (1996). Here we briefly sum up the main features. In order to solve the inversion problem, we model the four basic parameters by cubic spline functions. The ion composition is modelled using the method of Oliver (1979). This function is close to the analytical model used by Cabrit and Kofman (1996) and to the model established by Lathuillère and Pibaret (1992). The "full profile" procedure performs a parametric optimisation of the model parameters in the least-square sense.

The model of Cabrit and Kofman (1996) is purely an analytical one, built in order to approximate the IRI and Lathuillère and Pibaret (1992) models, the latter being obtained from previous EISCAT measurements and modelled by the hyperbolic tangent function. In Oliver's work, the model was based on a physical consideration using the continuity equation in a steady state. Oliver (1979) showed that the ion molecular composition can be well approximated by the following formula:

$$p = 1 - \frac{2}{1 + \sqrt{1 + \frac{8n(z)}{n(z_{50})}} \exp\left(t_{050} \times \left(\frac{P(z)}{P(z_{50})} - 1\right)\right)}, \quad (1)$$

where $z_{50}$ is the altitude for which $p(z_{50}) = 0.5$, $t_{050}$ is the bulk optical depth parameter at an altitude of $z_{50}$, $n(z)$ is

the density of the hypothetical neutral component and $P(z)$ is its pressure.

Instead of using a component with an hypothetical mass, we used the mean neutral density according to the formula:

$$n(z) = \frac{n_0 \times 16 + n_{02} \times 32 + n_{N_2} \times 28}{76} \quad . \tag{2}$$

The pressure was calculated by $P(z) = n(z) \cdot kT(z)$. In order to simplify our model, which cannot depend on too many parameters, we used the hydrostatic equation for the neutral densities.

$$n(z) = n_0 \frac{T_0}{T(z)} \exp\left(-\int_{z_0}^{z} \frac{\mathrm{d}z_1}{H(z_1)}\right) \quad , \tag{3}$$

$$H(z) = \frac{kT(z)}{mg} - \text{the scale height,}$$

and for neutral temperatures the Bates profile

$$T(z) = T_\infty - (T_\infty - T_0)\exp(-s(z - z_0)) \quad , \tag{4}$$

where $z_0 = 100$ km, $n_0$ – the neutral density at $z_0$, $T_0$ – the temperature, $m$ is the mass of the neutral component and $k$ is Boltzman's constant.

In our model we took $n_0$ from the MSIS 90 model: $T_\infty = 900$ K, $T_0 = 200$ K and $s = 0.03$. These values were chosen to be as close as possible to the neutral atmosphere given by MSIS 90, but of course the profiles obtained with the hydrostatic Eq. (3) are quite different from the profiles given by the MSIS model. The difference between the ion composition profile $p(z)$ given by Eq. (1), in which the neutral atmosphere is given by Eqs. (2), (3) and (4) and $p(z)$ calculated with the neutral atmosphere obtained with the MSIS 90 model is shown in Fig. 1. We plot in a continuous line the ion composition profile obtained with the MSIS 90 model with $z_{50} = 200$ km and $t_{050} = 1.5$, and two profiles using approximating formulas for the neutral component with $z_{50} = 200$ km and $t_{050} = 1.5$ and 0.8. One can see that the curve for $t_{050} = 0.8$ is close to the one using the MSIS 90 model. The plots clearly show that our modelling is adequate. Therefore, in our analysis we use Eqs. (1)–(4).

Oliver's model was derived for daytime photochemical equilibrium conditions. The applicability of this model for night-time conditions is not demonstrated. We use this model because the functional form is close to previously used models (Lathuillère and Pibaret, 1992, Cabrit and Kofman, 1996) and there is a theoretical justification for sunny atmosphere. In addition, during night conditions, precipitations produce ionisation. In particular, the physical sense of the $t_{050}$ parameter during the night is only related to the width of the profile and not to the optical depth.

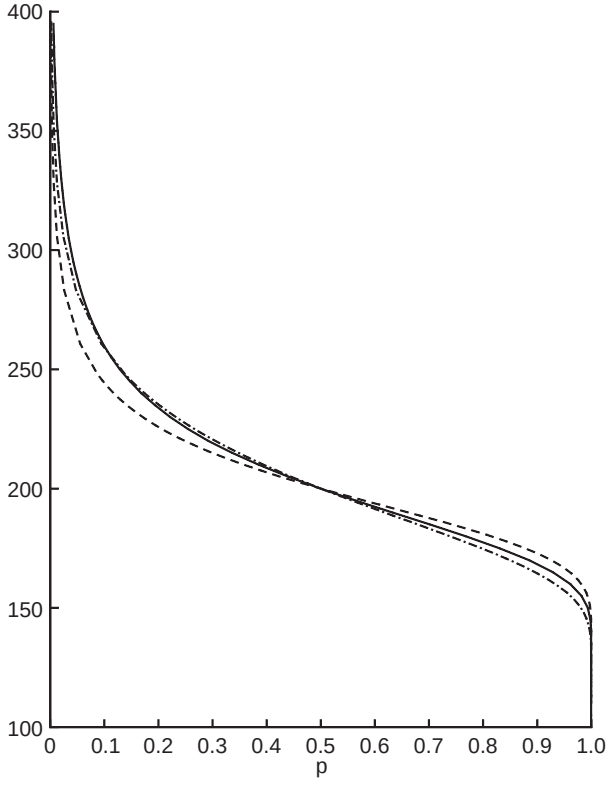


**Fig. 1.** The ion composition profile $p(z) = 1 - \frac{O^+}{n_e}$ calculated by Eq. (1), using the neutral atmosphere from the MSIS 90 model (*continuous lines*) and $z_{50} = 200$, $t_{050} = 1.5$, and our modelling for $z_{50} = 200$, $t_{050} = 1.5$ (*dotted lines*) and $z_{50} = 200$, $t_{050} = 0.8$ (*dash-dotted lines*)

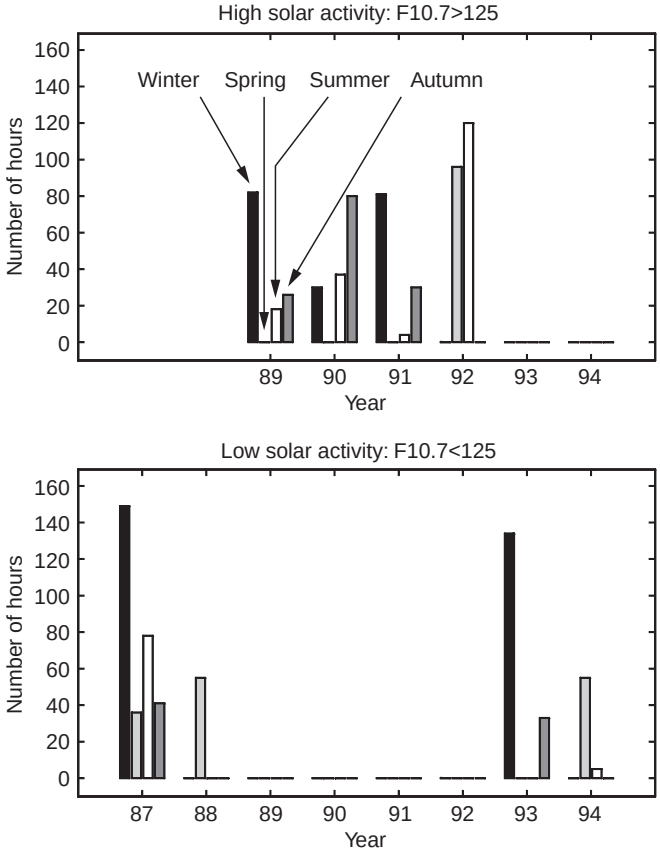


**Fig. 2.** The histogram of the whole set of analysed data in this paper

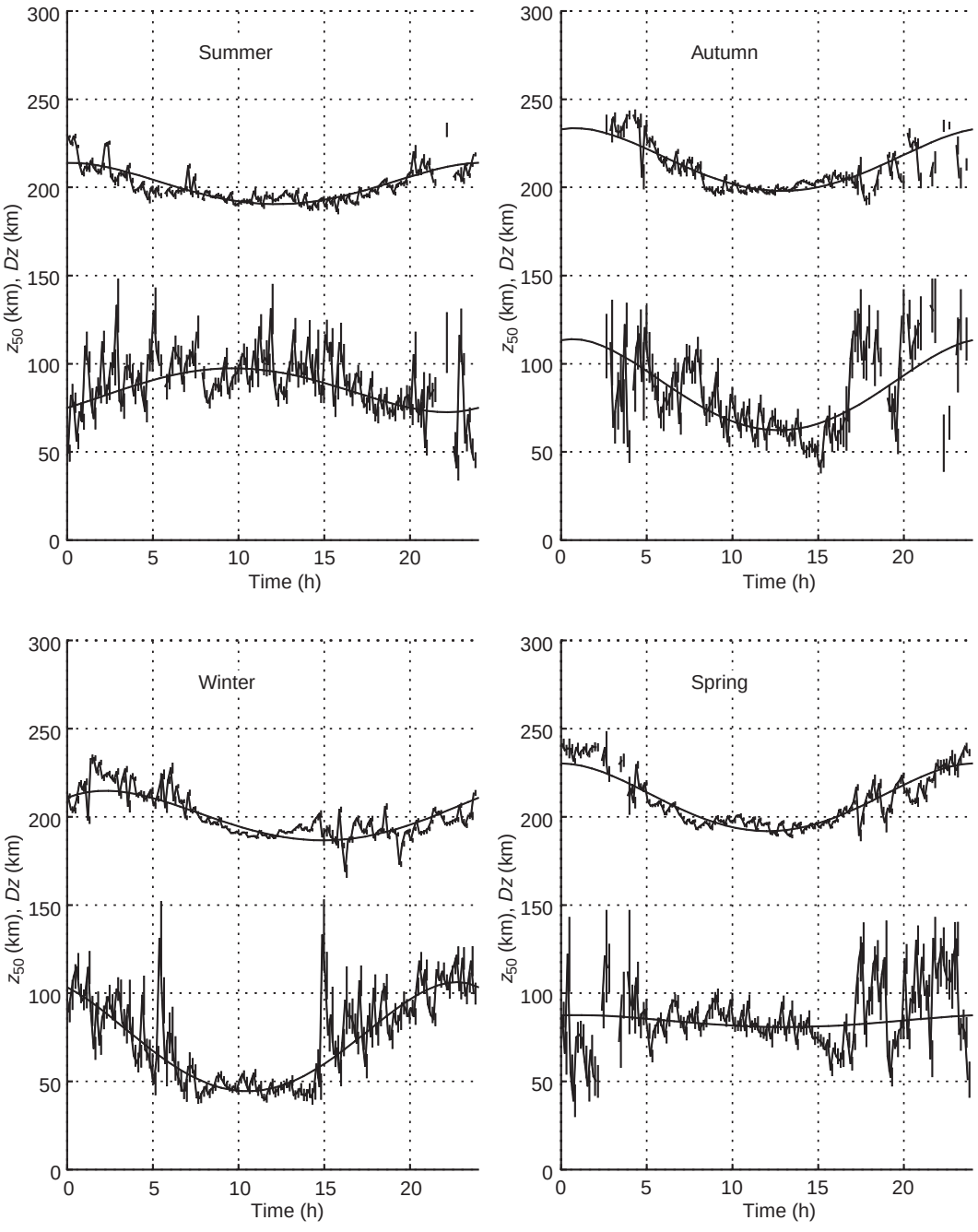


**Fig. 3.** The averaged values of parameters $z_{50}$ (*upper lines*) and *dz* (*lower lines*) for four seasons for low solar activity. The data were averaged in 10-min bins and are shown with their errors. The *smooth lines* represent the polynomial fit

### *2.2 Initial conditions for the fit*

In order to process a large amount of data, one had to solve the following problem: how to find the correct initial values. Simulations show that, with the functional dependence of the composition we are using, there is only one minimum of the mean quadratic error between the parametric data model and synthetic data. This is basically different from the existence of two minima in the classical gate-by-gate least-square fitting discussed in the introduction (see also Fig. 1 in Lathuillère and Pibaret, 1992). Actually, when one uses real data, there are rather often two local minima, especially during the night period when the signal-to-noise ratio is small. This anomalous behaviour is due to a few technical reasons: the adjustment (calibration) between the various types of correlation function measurements (long-pulse – multi-pulse or long-pulse – alternating code) or the approximation used in the ambiguity function calculation which assumes the ideal rectangular transmitted impulse and the constant gain may not be precise enough. Depending on the initial conditions, the fit converges on one or the other solution (local minimum). Hopefully, one of these solutions can be rejected because

it corresponds to non-monotonic electron and ion temperature profiles, which is unacceptable for data gathered during quiet ionospheric conditions. The other solution corresponds to smooth profiles and is considered to be the correct one.

For the automatic analysis of large amounts of data, we used the following strategy to select the "correct" solution:

1. One starts with fixed initial conditions ($z_{50} = 200$ and $t_{050} = 0.5$).
2. If the results of d$z$ are smaller than the value of 125 km, and the fit quality, which is the sum of the quadratic distance between measured and theoretical ACFs normalised by variances of each lag (see Cabrit and Kofman, 1996) is less than 1.5 and errors on the parameters are smaller than 30%, the results are taken as definitive. If not, the analysis is restarted with $z_{50}$ increased and decreased by steps of 10 km and $t_{050} = 1.5$.
3. If the results are correct, the values are used as initial conditions for the next fit. If not, one starts with the fixed initial conditions defined in point 1.

At the end of the analysis, the data are synthesised, and if one finds $z_{50}$ at too low altitudes for a long-time

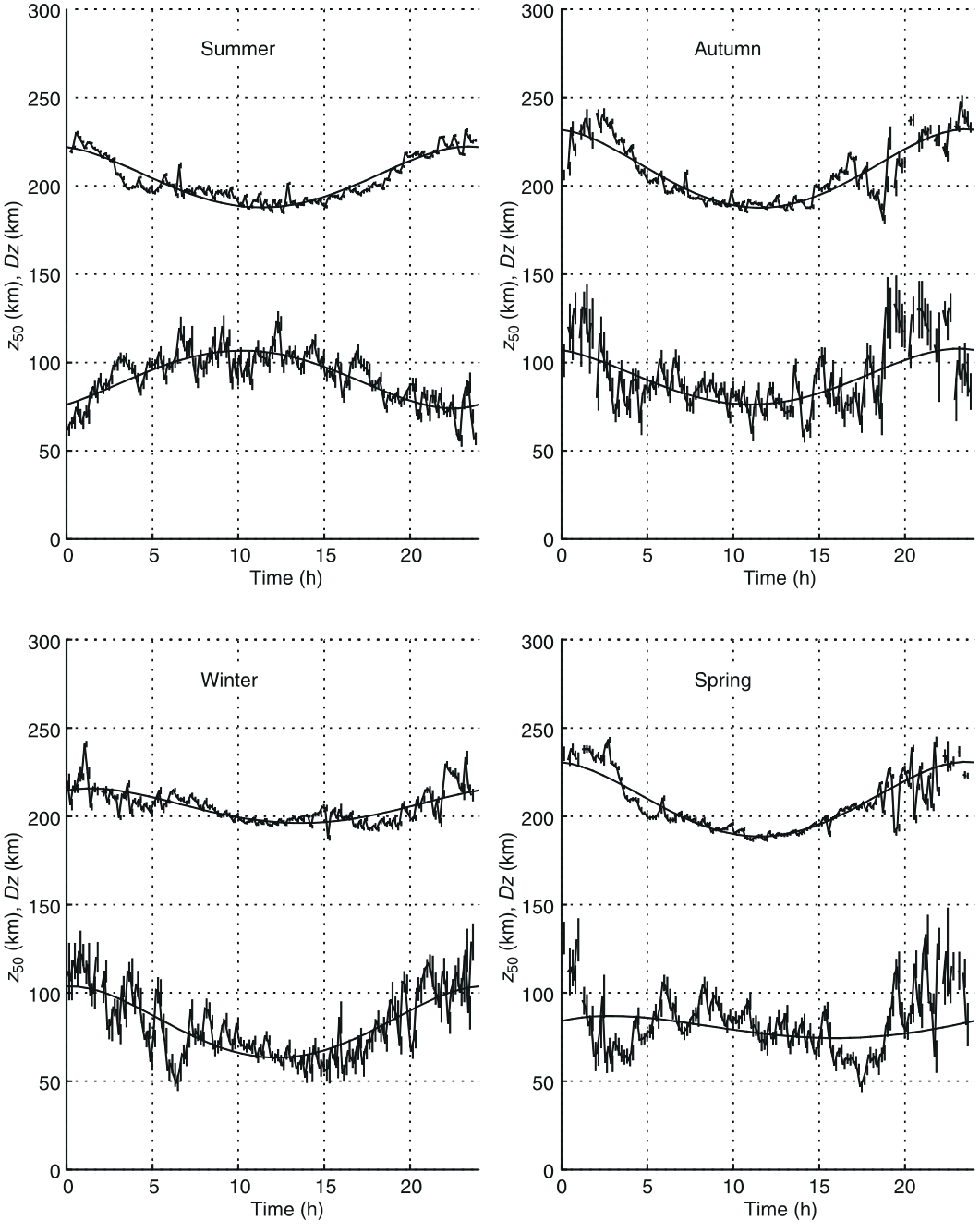


**Fig. 4.** As for Fig. 3 but for high solar activity

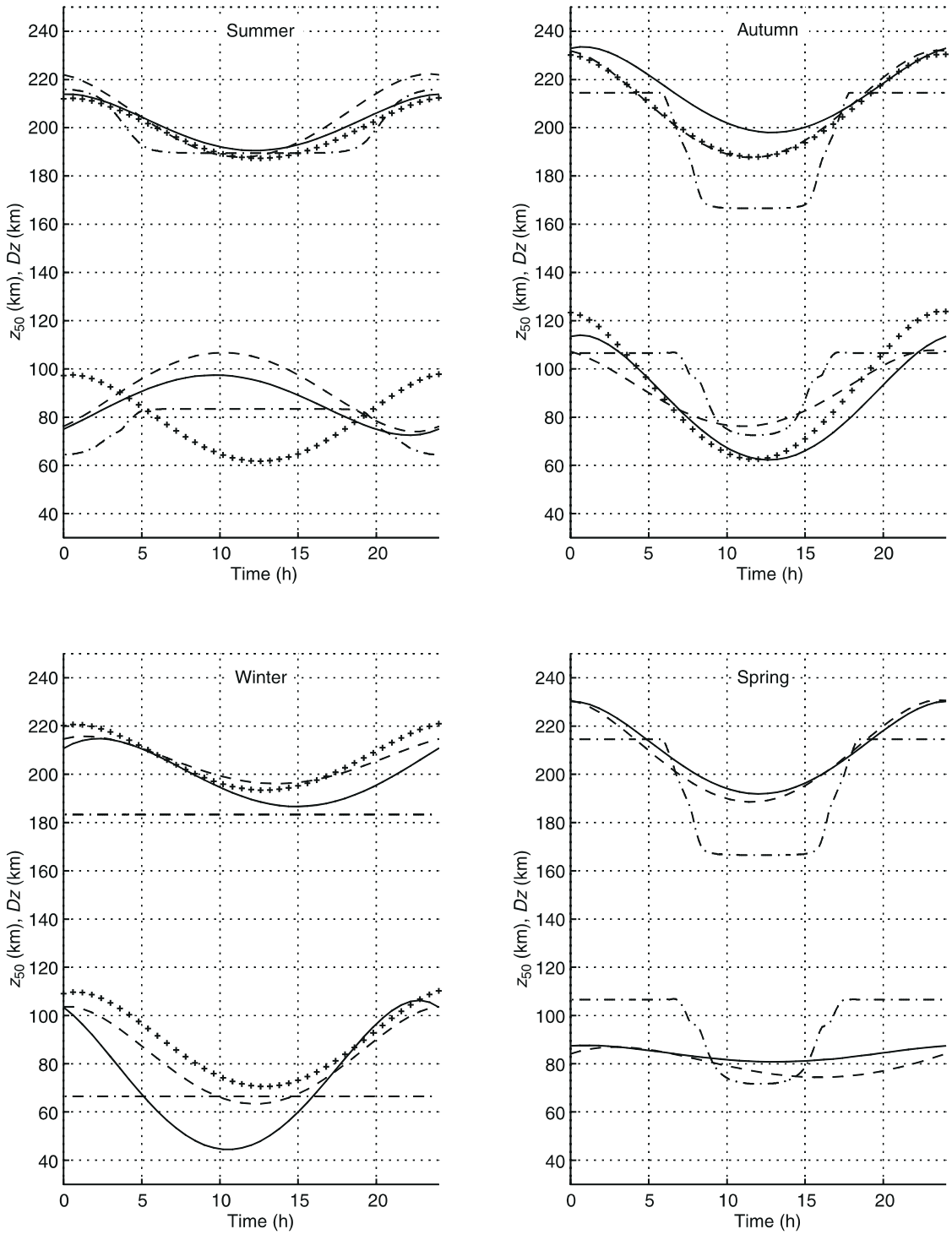


**Fig. 5.** The results of fitting for various seasons and high (*dashed line*) and low (*continuous line*) solar activity are shown. The *crossed line* corresponds to Lathuillère and Pibaret's model (there is no model for spring). The *dash-dotted* line corresponds to the IRI model for $100 < F10.7 > 200$

interval or $T_i$ profile with non-monotonic behaviour for many hours, we restart the analysis changing the initial conditions and using the daily model of Lathuillère and Pibaret (1992) for $z_{50}$ and $t_{050} = 1.5$. Because of these difficulties, we had to reanalyse about one half of the data for high solar activity periods. It is clear that we should avoid using the fixed model for the initial conditions to diminish the possibility of influence of the model on the results. We performed the statistical analysis of the data twice: once using all the results, and once excluding the results which were obtained with the initial conditions from the model. The results of the statistical analysis were the same.

### *2.3 Statistical analysis*

We analysed a large amount of EISCAT data dating from 1987 to 1994. The CP1 and CP2 data were analysed with the multi-pulse and long-pulse, and alternating code and long-pulse measurement techniques. The data were split into two sets, one corresponding to high solar activity with $F10.7 > 125$ and the other to low solar activity for $F10.7 < 125$. The data were selected as a function of the seasons; winter and summer were defined as 2 months before and 2 months after the solstices and spring and autumn as 1 month before and one after the equinoxes. This season definition is identical to the one made by Lathuillère and Pibaret (1992). This choice is also justified by the solar zenith angle variability during the various seasons. However, the choice of the season duration leads to a smaller amount of data for spring and autumn.

In Fig. 2 we show the histogram of analysed data for high and low solar activity. The aim of the statistical analysis is to obtain the average model of ion composition for each season as a function of UT. The averaged data were fitted with the fourth-order polynomial with continuity conditions on the polynomial and its derivatives at 0 UT. We also averaged the other ionospheric parameters $n_e$, $T_e$, $T_i$ and $v_i$.

As we explained before, we have only built the model for geophysical conditions without large electric field. In order to do so, we had to eliminate the data corresponding to periods of large electric field, larger than 25 mV/m. For a larger electric field, the ion velocity distribution starts to be non-Maxwellian and the analysis is no longer valid (Saint Maurice and Schunk, 1979; Gaimard *et al.*, 1996). When measurements of the electric field were not available, we used the ion temperature at 130 km as a selection criterion. The large ion temperature at 130 km indicates the Joule heating present in the ionosphere and through this the presence of the electric field. When the ion temperature was larger than 700° K, we rejected the data.

Once the data were selected, they were gathered in bins of 10 min as a function of the time (UT) for each season separately. The averages for all parameters $z_{50}$, d$z$, $n_e$, $T_i$, $T_e$ and $v_i$ were calculated. The weighted averages were made. The $z_{50}$, d$z$ and $t_{050}$ parameters were fitted by the polynomial as we explained before. In Figs. 3 and 4, we show the $z_{50}$, and d$z$ parameters for four seasons for low and high solar activity. The averaged points with their errors are shown with a 10-min time-resolution. The continuous lines correspond to the polynomial fit. The most striking feature is the correlation and the anti-correlation of two parameters ($z_{50}$ and d$z$) as a function of time. In summer, the two parameters are anticorrelated and in winter they are correlated. This behaviour is the same for high and low activity. The transition between these two behaviours is clearly seen for spring, but is weaker for autumn. For all seasons, one observes the minimum of the parameter $z_{50}$ at about noon. This was observed in the paper by Lathuillère and Pibaret (1992). The amplitude of the daily variation is smaller in winter and the minimum for winter is shifted by 2–3 h to the afternoon. The minimum of $z_{50}$ is at about 180 km for $F10.7 < 125$ and at about 200 km for $F10.7 > 125$. For autumn, the behaviour of the measurements is opposite to their behaviour for winter: $z_{50}$ is minimum at about 200 km for $F10.7 < 125$ and at about 190 km for $F10.7 > 125$. For summer and spring, there are no large differences for the altitude of the minima for low and high solar activity.

We gathered the results for low and high solar activity and compared them with those of the IRI model and Lathuillère and Pibaret (1992). In Fig. 5 we plotted (crosses) $z_{50}$ and d$z$ obtained by Lathuillère and Pibaret (1992) compared to our results. In general, the $z_{50}$ parameters show the same form. The striking feature is that our modelling corresponding to $F10.7 < 125$ (continuous line) is close to the modelling of Lathuillère and Pibaret (1992) for summer and the modelling corresponding to $F10.7 > 125$ (dashed line) is close to Lathuillère and Pibaret's one for autumn. The reason is that the measurements analysed in Lathuillère and Pibaret (1992) are averaged independently on the solar activity and the distribution of these measurements is not uniform. What happened is that there were more data during low solar activity for summer (about twice the amount of data used in averaging coming from low activity than from high activity) and about the same amount of data during high and low solar activity for autumn (private communication from Pibaret). The width (d$z$) of the profiles was analysed by Lathuillère and Pibaret globally, all data together. The authors searched for a linear dependence of the width (d$z$) on $z_{50}$, and this is why d$z$ has the same form for all seasons, like $z_{50}$ (except for spring, where there are no data). There are differences with our results especially for summer. The overall behaviour is different. We think that this is due to two reasons. The first is that all seasons were mixed and analysed together to find a linear dependence between d$z$ and $z_{50}$ (the data are very scattered, see Fig. 9 in Lathuillère and Pibaret). The second is that Lathuillère and Pibaret (1992) used plasma parameters inferred from a coarse-resolution (40 km), long-pulse data. Since the width of the transition region between molecular and atomic ions is of the same order as the spatial resolution, one can have some doubts regarding the behaviour of d$z$. In Fig. 6, we compare our profile obtained with Oliver's approximation (1979) with the profile of Lathuillère and Pibaret (1992) and the profile of the IRI model. This figure shows that Lathuillère and Pibaret's model and the results of this paper are different, especially for summer. This reflects the previous discussion. The behaviour of Lathuillère and Pibaret's model for altitudes under $z_{50}$ is determined by assumed symmetry. In fact, there are no measurements (or few) for these altitudes in their modelling due to the use of long-pulse data.

One can say that the IRI model (Fig. 5) behaves similarly, but of course the IRI model, as an average model built from a small amount of data, cannot reflect the measurements. The most striking feature is

the constant of $z_{50}$ and d$z$ as a function of time for winter, which is clearly different from our measurements.

In Table 1 (see Appendix), we give the coefficients of the fitted parameters ($z_{50}$, $t_{050}$ and d$z$) of the fourth-order polynomial:

$$P(t) = f1 + f2\left(\frac{t}{12}\right) + f3\left(\frac{t}{12}\right)^2 + f4\left(\frac{t}{12}\right)^3 + f5\left(\frac{t}{12}\right)^4$$

with $t$ ranging from 0 to 24. This table allows the generation of the model and its implementation.

## 3 Discussion of results

Some of the general characteristics of the temporal and seasonal behaviour described in the previous section can easily be explained with the simplified steady-state model of chemical reactions in the F1 region of the ionosphere. The presence of the minimum of the transition altitude ($z_{50}$) between molecular and $O^+$ at noon has two main causes.

The increase in electron density due to the decrease in the solar zenith angle will act on two reactions ($O^+ + N_2 \rightarrow NO^+ + N$, $NO^+ + e \rightarrow N + O$). The rate of the first one is proportional to the electron density, while the rate of the second one increases with its square.

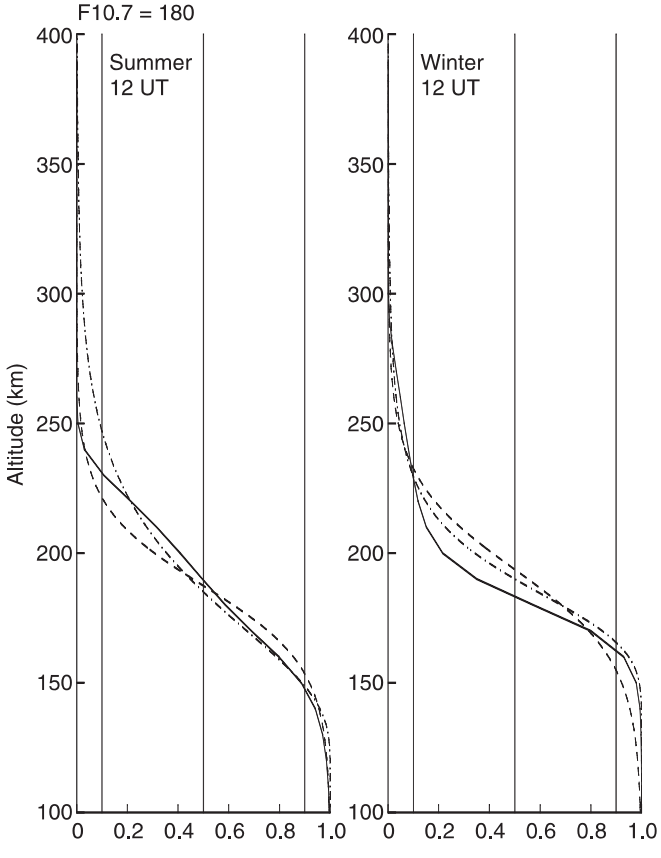


**Fig. 6.** The profiles modelled in this work (*dash-dotted line*) for high solar activity for winter and summer compared to the IRI model (*continuous line*) and to Lathuillère and Pibaret's (1992) model (*dashed line*)

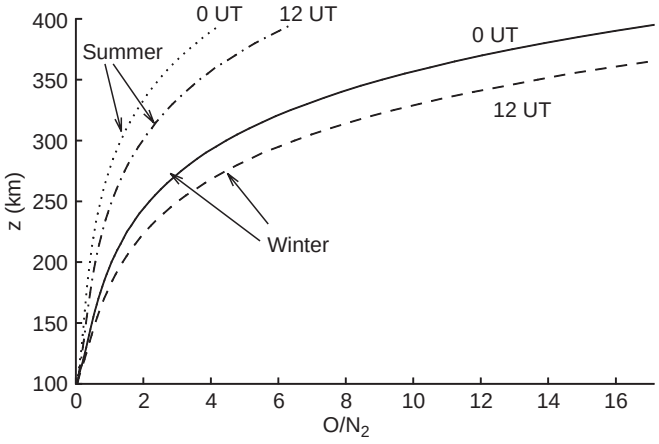


**Fig. 7.** The ratio $O/N_2$ for the summer and winter periods at noon and midnight obtained from the MSIS model

Therefore, for a given altitude, when the electron density increases, the density of $NO^+$ decreases comparatively to $O^+$ density and the result is the decrease in $z_{50}$.

The second cause of the decrease in $z_{50}$ is the increase in the $O/N_2$ ratio for all seasons at noon. In Fig. 7 we plot this ratio as a function of the altitude obtained from the MSIS 90 model. This increase will change the rate of ionisation of the atomic oxygen comparatively to the reaction $O^+ + N_2 \rightarrow NO^+ + N$, and this will increase the relative ratio between $O^+$and $NO^+$. In addition, the increase in the $O/N_2$ ratio modifies the abundance of $NO^+$ via the ionisation of $N_2$ and the reaction $N_2^+ + O \rightarrow NO^+ + N$, because the last reaction is the major loss for $N_2^+$ ions and the major source for $NO^+$.

The observed decrease in the altitude minimum of $z_{50}$ in winter for low solar activity comparative to high solar activity can also be explained by the behaviour of the $O/N_2$ ratio. The $O/N_2$ ratio at 200 km for low solar activity is larger than for high solar activity at noon and this is why the altitude of the minimum increases for high solar activity.

It is much more difficult to explain in a simple way the daily behaviour of the width of the ion composition profile d$z$. As we said before, we created an average model of measured ionospheric parameters according to seasons. In Fig. 8, we show the profiles of electron density for three seasons. To discuss the variability of d$z$, we will use these profiles. For winter, the decrease in d$z$ in the middle of the day means that the changes in the ionosphere are faster when altitude increases. This implies that the gradients of the ionospheric parameters which make the transition to $O^+$ should be stronger.

The major ionospheric parameters which influence this transition are, as stated in the foregoing discussion, the electron density and the ratio of $O/N_2$. In Fig. 8 we can see that for winter conditions, the electron density increases very fast at noon and at midnight the gradient is even negative at altitudes of interest. The fact that the electron density is larger in the E and F1 regions in winter at midnight than at noon is due to the fact that our model includes data during precipitation events. The

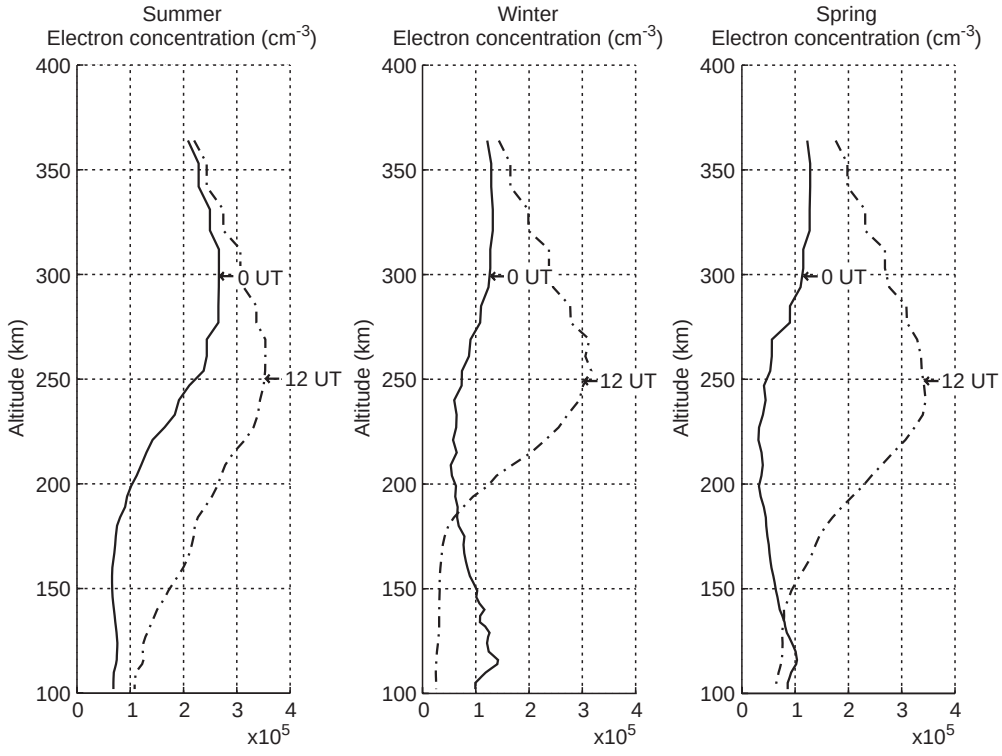


**Fig. 8.** The average ionospheric density at noon and midnight for low solar activity for three seasons

$O/N_2$ ratio also has a larger gradient at noon than at midnight (see Fig. 7). This explains the behaviour of the d$z$ parameter during winter.

The increase in d$z$ during the day and the anti-correlation with $z_{50}$ for summer is even more difficult to explain. In Fig. 8 one can see that the gradients of electron density at 0 UT and 12 UT are not too different. Therefore, the influence of these gradients is less important and different causes lie at the origin of the d$z$ behaviour. We think that the influence of the differences in the ion production at 0 UT and 12 UT are responsible for this behaviour.

## 4 Conclusion

In this short paper, we show the results of the analysis of 7 years of EISCAT data. Using a new method of data analysis we were able to build a seasonal model of ion composition in the F region of the ionosphere. We built a model for quiet ionospheric conditions, the word quiet corresponding to the absence of electric field in EISCAT measurements. In this sense our model is local, because the measurements came from the ionosphere above EISCAT. This is one of the reasons why our results are quite different from the non-local IRI model.

The comparison in Figs. 5 and 6 with the IRI model shows similarities in the shape (except in winter) of $z_{50}$ and d$z$ parameters, but the values and the exact behaviour are really different. The profiles (see Fig. 6) are quite different. The main reason for these differences comes from the fact that the IRI model is built on a small number of measurements of the composition especially for the auroral zone.

Compared with Lathuillère and Pibaret's work, we obtained different seasonal variations of the behaviour of the composition parameters, mainly for the width of the transition region between molecular and atomic ions. We believe in our result because the spatial resolution of our "full profile" analysis is much better than the resolution of Lathuillère and Pibaret's analysis and because our method is free from gradient effects.

We proposed a qualitative explanation of the temporal behaviour of the transition altitude ($z_{50}$) between molecular and atomic ions and the width (d$z$) of the composition profile which supports our results. The correlation and anti-correlation between these two quantities are explained by the gradients of electron density and of ion production. This explanation needs to be confirmed by a more precise simulation which includes the non-steady-state simulations of the auroral ionosphere, including the vertical and horizontal transport.

In conclusion, we think that we improved experimental models of ion composition in the auroral region. Our model is available on the EISCAT data-base web server and is ready to be used in incoherent-scatter data analysis.

*Acknowledgements* We thank Chantal Lathuillère for fruitful discussion and Béatrice Pibaret for her help. We also would like to thank the EISCAT Scientific Association for providing data. EISCAT is an international facility supported by the research councils of Finland, France, Germany, Japan, Norway, Sweden, and the UK.

Topical Editor D. Alcaydé thanks A. Huuskonen and another referee for their help in evaluating this paper.

**Appendix**

| | $f(1)$ | $f(2)$ | $f(3)$ | $f(4)$ | $f(5)$ |
|---|---|---|---|---|---|
| $F10.7 > 125$ | | | | | |
| $z_{50}$ | | | | | |
| winter | 214.67 | 19.87 | −101.27 | 81.40 | −17.87 |
| spring | 230.57 | −13.10 | −147.97 | 161.08 | −41.91 |
| summer | 221.94 | −14.82 | −113.54 | 128.36 | −33.94 |
| autumn | 231.87 | −14.10 | −155.31 | 169.41 | −44.12 |
| $F10.7 > 125$ | | | | | |
| $dz$ | | | | | |
| winter | 103.65 | 6.36 | −170.75 | 164.39 | −40.30 |
| spring | 84.12 | 25.83 | −68.62 | 42.79 | −7.47 |
| summer | 76.13 | 36.61 | 62.03 | −98.64 | 29.24 |
| autumn | 107.15 | −19.76 | −92.48 | 112.24 | −30.53 |
| $F10.7 > 125$ | | | | | |
| $t_{050}$ | | | | | |
| winter | 0.3689 | −0.00291 | 4.8244 | −4.8215 | 1.205 |
| spring | 0.7535 | −0.2540 | 2.355 | −2.101 | 0.4936 |
| summer | 0.9641 | −0.4858 | −1.016 | 1.5017 | −0.4361 |
| autumn | 0.4530 | 0.8011 | 1.011 | −1.812 | 0.5532 |
| $F10.7 < 125$ | | | | | |
| $z_{50}$ | | | | | |
| winter | 210.7 | 47.07 | −155.14 | 108.07 | −21.133 |
| spring | 230.2 | 1.525 | −155.75 | 154.21 | −38.361 |
| summer | 213.9 | 3.432 | −98.67 | 95.24 | −23.382 |
| autumn | 232.9 | 20.46 | −168.85 | 148.39 | −34.54 |
| $F10.7 < 125$ | | | | | |
| $dz$ | | | | | |
| winter | 103.4 | −58.04 | −141.66 | 199.71 | −57.182 |
| spring | 87.4 | 4.88 | −33.31 | 28.43 | −6.497 |
| summer | 75.0 | 34.79 | 30.54 | −65.33 | 20.680 |
| autumn | 113.4 | 23.43 | −238.35 | 214.92 | −50.800 |
| $F10.7 < 125$ | | | | | |
| $t_{050}$ | | | | | |
| winter | 0.24689 | 1.5307 | 5.613 | −7.144 | 1.9774 |
| spring | 0.61917 | 0.2996 | 1.183 | −1.483 | 0.4082 |
| summer | 1.1633 | −0.6438 | −0.726 | 1.370 | −0.4231 |
| autumn | 0.1254 | −0.394 | 6.239 | −5.846 | 1.412 |

## References


**Cabrit, B., and W. Kofman,** Ionospheric composition measurement by EISCAT using a global-fit procedure, *Ann. Geophysicae*, **14,** 1496–1505, 1996.

**Gaimard, P., C. Lathuillère and D. Hubert,** Non-Maxwellian studies in the auroral F region: a new analysis of incoherent-scatter spectra, *J. Atmos. Terr. Phys.*, **58,** 415–433, 1996.

**Gaimard, P., J. P. Saint Maurice, C. Lathuillère, and D. Hubert,** On the improvement of analytical calculations of auroral ion velocity distribution using recent Monte Carlo results, *J. Geophys. Res.*, in press, 1998.

**Holt, J. M., D. A. Rhoda, D. Tetelbaum, and A. P. Van Eyken,** Optimal analysis of incoherent-scatter radar data, *Radio Sci.*, **27,** 345–348, 1992.

**Hubert, D., and E. Kinzelin,** Atomic and molecular ion temperatures and ion anisotropy in the auroral F region in the presence of large electric fields, *J. Geophys. Res.*, **97,** 1053–4059, 1992.

**Lathuillère, C., and B. Pibaret,** A statistical model of ion composition in the auroral lower F region, *Adv. Space Res.*, **12,** 147–156, 1992.

**Lathuillère, C., G. Lejeune, and W. Kofman,** Direct measurements of ion composition with EISCAT in the high-latitude F1 region, *Radio Sci.*, **18,** 887–893, 1983.

**Lethinen, M. S., A. Huuskonen, and J. Pirttilä,** First experiences of full-profile analysis with GUISDAP, *Ann. Geophysicae*, **14,** 1487–1495, 1996.

**Moorcroft, D. R.,** On the determination of temperature and ionic composition by electron backscattering from the ionosphere and magnetosphere, *J. Geophys. Res.*, **69,** 955–970, 1964.

**Oliver, W. L.,** Incoherent-scatter, radar studies of daytime middle thermosphere, *Ann. Geophys.*, **35,** 121–139, 1979.

**Petit, M.,** Application de la diffusion "quasi-incoherent" à la mesure de la température, de la composition ionique et de la concentration électronique de l'ionosphère, *Ann. Geophys.*, **19,** 63–71, 1963.

**Saint Maurice, J.-P., and R. W. Schunk,** Ion velocity distributions in the high-latitude ionosphere, *Geophys. Space Phys.*, **17,** 99–134, 1979.